RSC Advances

PAPER

View Article Online
View Journal | View Issue

Cite this: *RSC Adv.*, 2021, **11**, 2167

Sensitive impedimetric detection of troponin I with metal–organic framework composite electrode†

Arushi Gupta,[ab] Sandeep Kumar Sharma,[c] Vivek Pachauri,[d] Sven Ingebrandt,[d] Suman Singh,[a] Amit L. Sharma[ab] and Akash Deep *[ab]

Received 1st August 2020
Accepted 17th December 2020

DOI: 10.1039/d0ra06665f

rsc.li/rsc-advances

Metal–organic frameworks (MOFs) are promising materials for biosensing applications due to their large surface to volume ratio, easy assembly as thin films, and better biocompatibility than other nanomaterials. Their application in electrochemical biosensing devices can be realized by integrating them with other conducting materials, like polyaniline (PANI). In the present research, a composite of a copper-MOF (*i.e.*, $Cu_3(BTC)_2$) with PANI has been explored to develop an impedimetric sensor for cardiac marker troponin I (cTnI). The solvothermally synthesized $Cu_3(BTC)_2$/PANI composite has been coated as a thin layer on the screen-printed carbon electrodes (SPE). This electroconductive thin film was conjugated with anti-cTnI antibodies. The above formed immunosensor has allowed the impedimetric detection of cTnI antigen over a clinically important concentration range of 1–400 ng mL^{-1}. The whole process of antigen analysis could be completed within 5 min. The detection method was specific to cTnI even in the co-presence of other possibly interfering proteins.

1. Introduction

Cardiovascular diseases are one of the major health problems.[1] Acute myocardial infarction (AMI), or more commonly known as the heart attack, is responsible for a large number of deaths around the globe. Electrocardiography, enzyme-linked immunosorbent assay (ELISA), and radioimmunoassay (RIA) are the generally used approaches for the diagnosis of AMI.[2–4] However, there is a need for the development of new rapid analysis methods for the timely detection of AMI. Biosensors (both electrochemical and optical) are the obvious choices because of their user-friendliness and fast response time. Biosensors are also useful to allow better disease management due to the advantages of low-cost and on-site detection capability.

The analysis of blood biomarkers is important to screen the AMI cases. Biomarkers are referred to as any substance, structure or biological process that can be measured in the body to help in the prediction of the outcome or disease. In healthy subjects, the biomarkers flow in the blood is regulated under certain limits. Any elevation/depression beyond those limits is taken as an indicator of the disease. Cardiac troponin I (cTnI) has been regarded as a Gold standard for the diagnosis of AMI. In the blood of a healthy human, cTnI biomarker is present in a level of ≤0.4 ng mL^{-1}.[5] An increase beyond the said value indicates the damage to the cardiac myocytes.[6] Therefore, the presence of high concentrations of cTnI in blood is associated with a high risk of heart attack.[7] cTnI is an important diagnostic parameter as it is specifically produced in the myocardium. Significant attention has been paid by the researchers in the recent past to develop electrochemical and fluorescent biosensors for the analysis of cTnI.[8–13] In particular, electrochemical biosensors provide better sensitivity and quantitative estimations while also requiring relatively fewer amounts of nanomaterials and recognition biomolecules during their fabrication.[14]

The performance of electrochemical biosensors is largely dependent upon the transducer surface. Graphene, carbon nanotubes (CNTs), conducting polymers, and silicon nanowires are the recently investigated popular transducer surfaces for the development of electrochemical biosensors for cTnI.[15–19] As advanced functional materials, the metal–organic frameworks (MOF) have garnered great interest in recent years because of their fascinating material properties.[20–24] MOFs have also been suggested useful for the development of electrochemical biosensors for different categories of analytes. For instance, Wang *et al.* have developed a sensor for the electrochemical detection of Cd^{2+} ions.[25] These authors used an electrode modified with a composite of UIO-66-NH_2 MOF with polyaniline (PANI) to obtain the detection of Cd^{2+} from 0.5–600 μg mL^{-1} with a limit of detection (LOD) of 0.3 μg mL^{-1}. Another MOF/PANI composite has been reported for the development of an aptasensor of *E. coli* O157:H7 within a range of 2.1×10^1 to 2.1

[a]*Central Scientific Instruments Organisation (CSIR-CSIO), Sector 30-C, Chandigarh, India. E-mail: dr.akashdeep@csio.res.in*

[b]*Academy of Scientific and Innovative Research (AcSIR-CSIO), Ghaziabad-201002, India*

[c]*Department of Physics, Sri Guru Gobind Singh College, Sector 26, Chandigarh, India*

[d]*IWE1-Institut für Werkstoffe der Elektrotechnik 1, RWTH Aachen University, Germany*

† Electronic supplementary information (ESI) available. See DOI: 10.1039/d0ra06665f

$\times 10^7$ cfu mL^{-1}.[26] A SiO_2-coated Cu-MOF has been reported for the detection of NH_3 from 1–100 mg L^{-1} (LOD = 0.6 mg L^{-1}).[27]

Due to their insulating property, the MOFs are often used in conjunction with other electrochemically active nanomaterials in order to design electrochemical biosensors. The use of composites of MOFs (*e.g.*, $Cu_3(BTC)_2$ in present study) with traditional conducting polymers adds some vital characteristics to the sensor surfaces. A large surface area and the availability of open metal sites contribute to an enhanced electrochemical activity. The MOF–polymer composite surfaces also deliver additional functional sites for the attachment of biomolecules. The porous MOFs can also play role in better diffusion of electrolyte ions across the circuit. In the present study, we report the application of a thin film of a MOF-conducting polymer (CP) composite to develop a highly sensitive electrochemical biosensor for cTnI. To the best of our knowledge, no previous report is available discussing the use of a MOF-CP composite for the electrochemical analysis of cTnI. A copper-based MOF, *i.e.*, $Cu_3(BTC)_2$, has been mixed with carboxyl functionalized polyaniline (c-PANI). The resulting composite was coated as a thin film over a screen-printed carbon electrode and subsequently bioimmobilized with anti-cTnI antibodies. The above prepared biosensor was used for the electrochemical impedance spectroscopy (EIS) based quantification of cTnI in both synthetic buffer and spiked mice serum samples. As the findings have highlighted, the present biosensing system gives fast response, wide range of detection, a low limit of detection, and specificity.

2. Experimental

2.1. Materials and equipment

All the reagents and solvents (analytical grade purity), including benzene-1,3,5-tricarboxylic acid (H_3BTC), copper nitrate ($Cu(NO_3)_2$), and polyaniline (PANI), used during the course of the study were purchased from Sigma (India). Cardiac troponin I (cTnI) antigen and anti-cTnI antibody were procured from MyBioSource (USA). The screen-printed carbon electrodes (SPEs) were obtained from Zensor. The structural and morphological studies were carried out with a field emission scanning electron microscope (FE-SEM, Hitachi, SU8010) and an X-ray diffractometer (Brooker D8 Advance, Kα = 1.54 Å). Fourier transform infrared (FTIR) and nitrogen isotherm analysis were performed on a PerkinElmer, Spectrum Two and a BELSORP-max (Microtrac) system, respectively.

2.2. Synthesis of carboxylated PANI, $Cu_3(BTC)_2$ and $Cu_3(BTC)_2$/PANI composite

Carboxylated polyaniline (c-PANI) was prepared by the chemical oxidation of aniline and 2-aminoterephthalic acid (0.07 : 0.03 M) with ammonium persulphate (0.1 M) in an acidic medium of 1 M HCl. The copolymerisation reaction was carried out in an ice bath (0 °C) under vigorous stirring (3 h). The prepared c-PANI was washed with 1 M HCl and then dried under vacuum (24 h).

$Cu_3(BTC)_2$ and $Cu_3(BTC)_2$/PANI composite were synthesized at room temperature (RT, 25 ± 2 °C) conditions by solvothermal method.[20] For the synthesis of $Cu_3(BTC)_2$, 0.5 g (2.38 mM) of H_3BTC and 1.05 g (4.34 mM) $Cu(NO_3)_2$ were dispersed in a solvent mixture of distilled water, ethanol and dimethylformamide (DMF) (1 : 1 : 1, 100 mL each). The reaction mixture was well mixed by stirring, followed by the slow addition of triethylamine (TEA, 0.5 mL). The contents were subject to bath sonication for 45 min, which resulted in the precipitation of blue crystals. The formed product was separated by centrifugation (10 000 rpm, 10 min), washed several times with water and ethanol, and finally dried in vacuum (at 70 °C). The synthesis of $Cu_3(BTC)_2$/PANI was also processed as per the above procedure. 100 mg of c-PANI was pre-mixed with H_3BTC and $Cu(NO_3)_2$ precursors, prior to the mixing and TEA addition steps. The synthesized composite product ($Cu_3(BTC)_2$/PANI) was washed several times with water and ethanol before drying overnight under vacuum conditions.

Note that different amounts of c-PANI (*e.g.*, 50 mg, 100 mg and 150 mg) were used to optimize the ratio of $Cu_3(BTC)_2$ and PANI in the $Cu_3(BTC)_2$/PANI composite. It was observed that low amount (50 mg) of PANI was not sufficient for attaining conducting films while higher amount (150 mg) was detrimental to the surface area property. Therefore, 100 mg PANI was selected as the optimum amount to be added during the synthesis of $Cu_3(BTC)_2$/PANI.

2.3. Modification of screen-printed carbon electrodes (SPEs) with $Cu_3(BTC)_2$/PANI and subsequent covalent attachment of anti-cTnI antibodies

10 μL ethanolic dispersions of $Cu_3(BTC)_2$/PANI (1 mg mL^{-1}) were drop casted on the working areas of several SPEs. A higher concentration of dispersion settled quickly and was not uniform. The composite modified electrodes were annealed at 90 °C for 4 h to guarantee a proper adhesion of the material over the SPE surface. The above step (drop-cast and annealing) was repeated to ensure uniformity of the film. Two-step drop casting and annealing process was found optimum as further layering did not change the charge transfer characteristics of the film as determined in some preliminary electrochemical studies. Next, the electrodes were incubated with a PBS (phosphate buffer saline, pH 7.4) solution of 0.05 M EDC [(1-ethyl-3-(3-(dimethylamino)propyl) carbodiimide] and 0.01 M NHS (*N*-hydroxysuccinimide) for 2 h. The above step was necessary for the activation of carboxyl groups before the attachment of antibodies. Thereafter, the electrodes (working area) were left in contact with the antibody solution (1 μg mL^{-1}) for 2 h. This dilution of the antibody was selected on the basis of earlier published immunosensing protocols. The prepared bio-electrodes were washed with PBS buffer before blocking the non-specific antibody binding sites with 0.01% Tween 20. Thus prepared Ab/$Cu_3(BTC)_2$/PANI biosensing electrodes were stored under refrigerated conditions.

2.4. Electrochemical impedance spectroscopic (EIS) analysis

EIS characteristics of the biosensor were studied in a ferro/ferri electrolyte solution (5 mM $K_3Fe(CN)_6$ + 5 mM $K_4Fe(CN)_6 \cdot 3H_2O$

in 0.1 M PBS). The frequency was varied within a range of 0.1 Hz to 1 MHz keeping the amplitude of 5 mV. Data were collected in form of Nyquist plots. Randles circuit was used for fitting and the calculation of charge transfer resistance (R_{ct}) values.[28,29] The Ab/$Cu_3(BTC)_2$/PANI electrodes were used for the analysis of a range of cTnI solutions (1–400 ng mL^{-1}). For this, 10 μL of the antigen solution was exposed to the Ab/$Cu_3(BTC)_2$/PANI electrodes and left to incubate for 5 min, unless otherwise mentioned. Subsequently, the electrode was washed and its EIS characteristics were recorded in the standard ferro/ferri electrolyte.

3. Results and discussion

3.1. Spectroscopic and structural characterization

Fig. 1 shows the FTIR and XRD analysis of $Cu_3(BTC)_2$, $Cu_3(BTC)_2$/PANI, and Ab/$Cu_3(BTC)_2$/PANI samples. In FTIR spectra of all the three sample (Fig. 1a), the 1618 and 1560 cm^{-1} bands corresponded to the asymmetric stretching of the linker component (BTC) of $Cu_3(BTC)_2$.[30,31] The band from benzene in BTC appeared around 1444 and 1374 cm^{-1} (stretching vibrations). A band at 492 cm^{-1} was associated with the Cu metal center.[32] The spectrum of $Cu_3(BTC)_2$/PANI was characterized with IR bands between 2500–3500 cm^{-1}, attributable to the

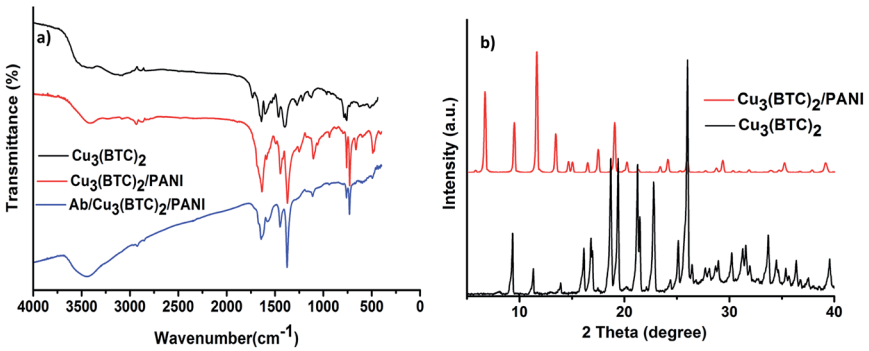

Fig. 1 (a) FTIR spectra of $Cu_3(BTC)_2$, $Cu_3(BTC)_2$/PANI, and Ab/$Cu_3(BTC)_2$/PANI; (b) XRD patterns of $Cu_3(BTC)_2$ and $Cu_3(BTC)_2$/PANI.

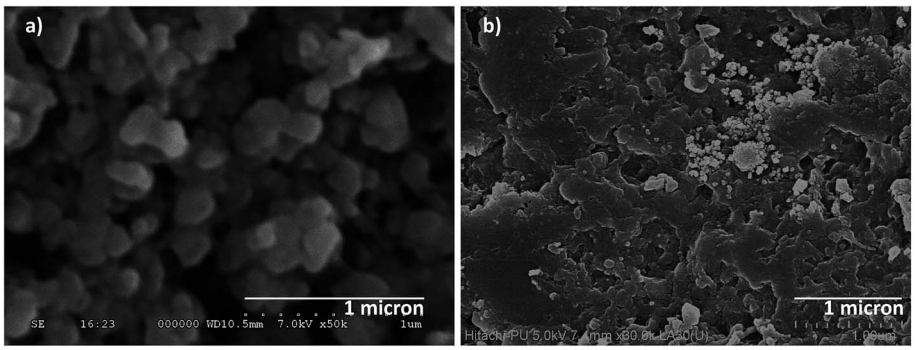

Fig. 2 FE-SEM of (a) $Cu_3(BTC)_2$; (b) $Cu_3(BTC)_2$/PANI.

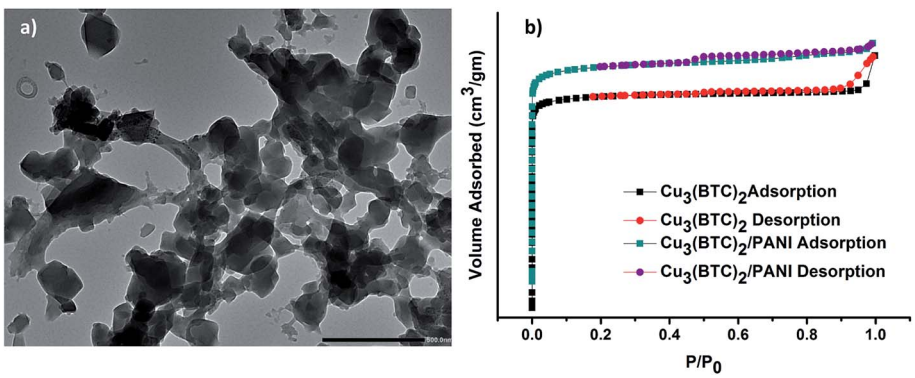

Fig. 3 (a) TEM image of $Cu_3(BTC)_2$/PANI; (b) N_2 adsorption–desorption isotherms for $Cu_3(BTC)_2$ and $Cu_3(BTC)_2$/PANI.

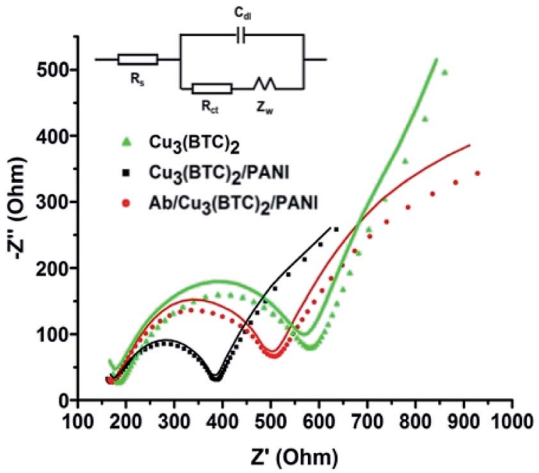

Fig. 4 Nyquist plots recorded for $Cu_3(BTC)_2$, $Cu_3(BTC)_2$/PANI, and Ab/$Cu_3(BTC)_2$/PANI electrodes during different stages of biosensor preparation. Experimental and fitted Nyquist plots are shown as dot and line curves, respectively.

N═H stretching vibration.[33] The presence of PANI was suggested by a band at 806 cm^{-1} (stretching vibration of C–N and out of plane bending of C–H).[34] FTIR spectrum of composite also showed bands of enhanced intensity at 1618 and 1516 cm^{-1}. As such, PANI related bands overlapped with other bands of $Cu_3(BTC)_2$. Nonetheless, these bands were stronger in the composite sample because of a successful incorporation of PANI. In case of Ab/$Cu_3(BTC)_2$/PANI, an extra peak was observed at 1640 cm^{-1}, pertaining to the N═C vibrations. This observation verified the binding of antibodies with the material.

The crystallinity of the synthesized $Cu_3(BTC)_2$ and $Cu_3(BTC)_2$/PANI samples was investigated with the XRD investigations (Fig. 1b). The spectra were characterized with peaks that matched well with the simulated XRD data and agreed with the literature reports. The main 2θ peaks in case of $Cu_3(BTC)_2$ can be mentioned as 5.8°, 9.5°, 11.6°, 13.5°, 19.8°, 25.3° and 29.4°.[35] Few of the small angle peaks were missing or having different intensities in the $Cu_3(BTC)_2$/PANI sample as a result of polymer mixing with the MOF structure.[26]

The FE-SEM micrograph of $Cu_3(BTC)_2$ and $Cu_3(BTC)_2$/PANI samples are presented in Fig. 2. $Cu_3(BTC)_2$ was formed in form of nanocrystals with size ranging 100–200 nm. A crystalline nature of the synthesized composite material was also evident. PANI structure has acted as a filler (thin film) for the MOF and helped in interconnecting the individual particles. Some white particles resembled $Cu_3(BTC)_2$ structure in the composite. In overall, thin film of PANI has embedded the MOF particles. Such a homogeneous thin film of MOF, after the mixing of PANI, is beneficial for the development of electrochemical biosensing surfaces. The TEM analysis of $Cu_3(BTC)_2$/PANI is

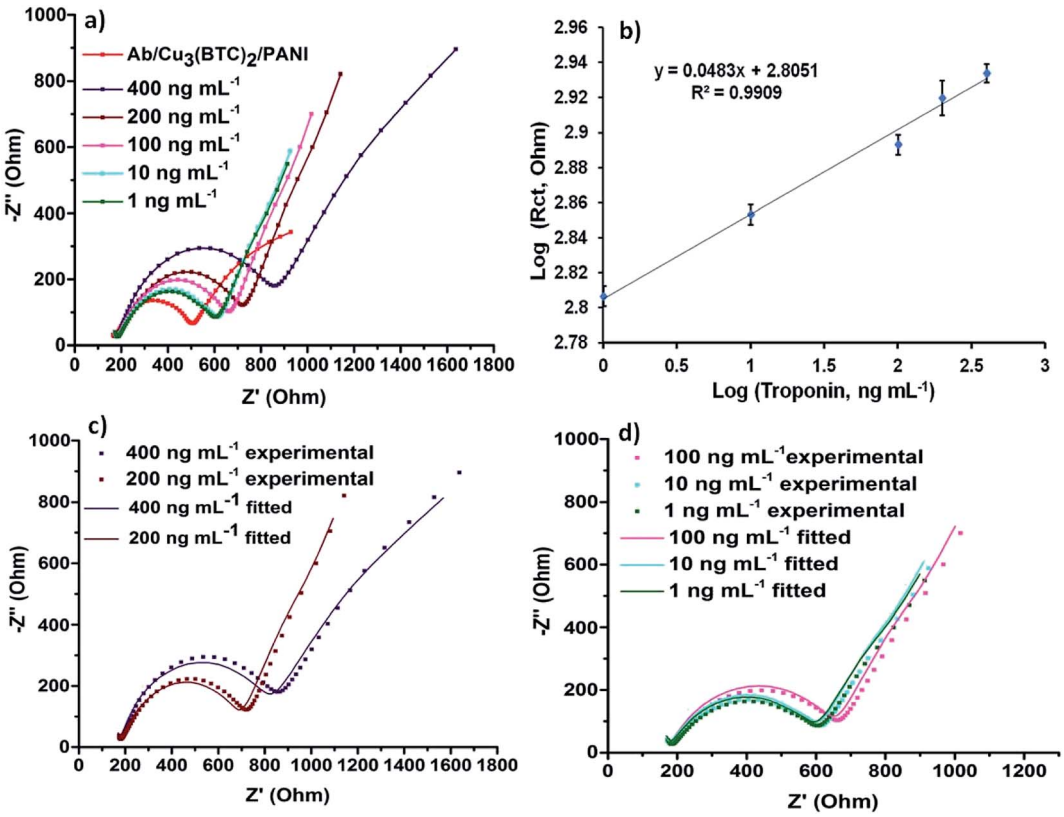

Fig. 5 (a) EIS response of Ab/$Cu_3(BTC)_2$/PANI biosensor toward different concentration of cTnI (1–400 ng mL^{-1}); (b) corresponding calibration plot between R_{ct} values and cTnI concentration; (c) experimental and fitted Nyquist plots for the response of Ab/$Cu_3(BTC)_2$/PANI sensor towards 400 ng mL^{-1} and 200 ng mL^{-1} cTnI; (d) experimental and fitted Nyquist plots for the response of Ab/$Cu_3(BTC)_2$/PANI sensor towards 100 ng mL^{-1}, 10 ng mL^{-1}, and 1 ng mL^{-1} cTnI.

presented in Fig. 3a. Compared to the TEM image of $Cu_3(BTC)_2$ alone (Fig S1, ESI†), the integration of two material components was evident in the $Cu_3(BTC)_2$/PANI structure. The thin film of PANI has connected the MOF particles.

N_2 absorption–desorption isotherms for the estimation of BET surface areas of materials are presented in Fig. 3b. The observed trends of both sorption–desorption curves were typical for the mesoporous materials.[36] The BET surface area of $Cu_3(BTC)_2$ was calculated to be 1102 $m^2\ g^{-1}$, which got reduced to 754 $m^2\ g^{-1}$ in case of $Cu_3(BTC)_2$/PANI. This limited reduction in the surface area of the composite, compared to the MOF alone, can also be taken as an indicator of a successful formation of the desired $Cu_3(BTC)_2$/PANI composite.

3.2. Application of Ab/$Cu_3(BTC)_2$/PANI biosensor for detection of cTnI

Electrochemical impedance spectroscopy (EIS) is one of the most widely used techniques to develop electrochemical immunoassays. EIS data is collected in the form of Nyquist plots, which compare out-of-phase component with the in-phase component. Nyquist plots are fit to the best circuit model to find out the values of important circuit components. Nyquist plots recorded for the $Cu_3(BTC)_2$, $Cu_3(BTC)_2$/PANI and Ab/$Cu_3(BTC)_2$/PANI modified SPEs are shown in Fig. 4. These plots have been obtained as semicircles and were fitted with Randles circuit (inset of Fig. 4). The actual data points and the fitted curve are also presented in Fig. 4. The data fitting allowed the estimation of circuit parameters like charge transfer resistance (R_{ct}) and double layer capacitance (C_{dl}).[37,38] A reduction in the semicircle diameter for the $Cu_3(BTC)_2$/PANI electrodes, compared to the $Cu_3(BTC)_2$ electrodes, provided an evidence that the overall resistance of the bare MOF experienced a significant attenuation once this material was mixed with PANI. The estimated values of R_{ct} also confirmed the same. Fig. 4a and b also shows the EIS data for the antibody modified $Cu_3(BTC)_2$/PANI electrodes (*i.e.*, Ab/$Cu_3(BTC)_2$/PANI). Due to the formation of protein layer, which was less conducting, the antibody modified electrodes again experienced an enhancement in the semicircle diameter and R_{ct} values.

The electrochemical changes in the EIS properties of Ab/$Cu_3(BTC)_2$/PANI) biosensing SPEs, as they were used for the analysis of different concentrations (1–400 ng mL^{-1}) of cardiac troponin I (cTnI) antigen, are presented in Fig. 5a. The experimental EIS data along with the respective fitted curves for the different concentrations are shown in Fig. 5c and d. An increase in the R_{ct} values was evident as a result of the antibody–antigen binding. This increase was proportional to the concentration of cTnI (Fig. 5b). The studies have highlighted the usefulness of the Ab/$Cu_3(BTC)_2$/PANI biosensor for the detection of cTnI over a wide and clinically significant range of analyte concentration. The limit of detection (LOD) was estimated based on the following expression:

$$\mathrm{LOD} = 3 \times \frac{\text{standard deviation at 1 ng mL}^{-1}\text{measurement}}{\text{slope of calibration curve}} \quad (1)$$

The LOD was calculated to be 0.8 ng mL^{-1}. We also investigated the minimum time required for the biosensor to show a stable response against cTnI. For this, 10 ng mL^{-1} of cTnI was left to incubate with the Ab/$Cu_3(BTC)_2$/PANI biosensor for different time durations. The EIS characterises were then measured in ferro/ferri electrolyte. This study was useful to

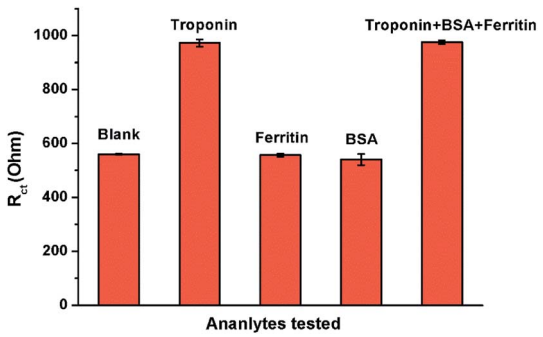

Fig. 7 Variation in the R_{ct} of Ab/$Cu_3(BTC)_2$/PANI biosensor against cTnI and some other non-specific analytes (cTnI = 400 ng mL^{-1}, BSA and ferritin = 500 ng mL^{-1}).

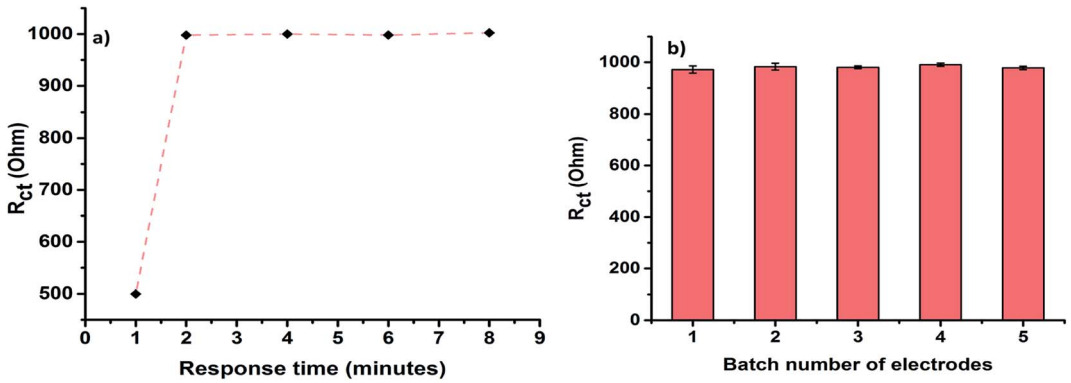

Fig. 6 (a) Response time of Ab/$Cu_3(BTC)_2$/PANI toward 10 ng mL^{-1} cTnI; (b) response of different batches of prepared Ab/$Cu_3(BTC)_2$/PANI biosensor toward 10 ng mL^{-1} cTnI.

Table 1 A summary of electrochemical sensors reported for the detection of cTnI[a]

S. no	Electrode material	Technique	LOD (ng mL^{-1})	Range of detection (ng mL^{-1})	Analysis time (min)	Ref.
1	CdS quantum dots	DPV	0.0011 ng L^{-1}	—	240	39
2	GMWCNT	Electrochemical	0.00094	0.001–10	—	15
3	COOH-CNT	Impedimetric	0.033	1–10	60	40
4	AuNP	Impedimetric	0.1	0.1–31.5	10	41
5	**$Cu_3(BTC)_2$/PANI**	**Impedimetric**	0.8	**1–400**	**2 (electrode–analyte incubation period), total analysis time is 10 min**	**Present work**

[a] DPV: differential pulse voltammetry; CdS: cadmium sulphide; GWCNT: graphene multiwalled carbon nanotubes; CNT: carbon nanotubes; AuNP: gold nanoparticles.

Table 2 Analysis of mice serum sample spiked with known concentration of cTnI with Ab/$Cu_3(BTC)_2$/PANI biosensor

Concentration of cTnI added (ng mL^{-1})	Response of biosensor (R_{ct})	Corresponding cTnI concentration as deduced for the standard calibration curve	Recovery %
100	776	102.2	102.2
50	741	50.4	100.8
5	683	5.02	100.4

establish a rapid response time (2 min) of the Ab/$Cu_3(BTC)_2$/PANI biosensor (Fig. 6a).

The studies have also been performed for deducing a comparison between the Ab/$Cu_3(BTC)_2$/PANI biosensor and a reference MOF free Ab/PANI biosensor. This comparative study has helped to investigate the effect of $Cu_3(BTC)_2$ on the sensor performance. The response of the reference Ab/PANI biosensor (R_{ct} *vs.* analyte concentration) is shown in Fig. S2.† The Ab/PANI biosensor did not detect cTnI below 50 ng mL^{-1}, suggesting that it does not have a good detection limit. In comparison to Ab/$Cu_3(BTC)_2$/PANI biosensor (0.85 Ω ng^{-1} mL^{-1}), the Ab/PANI showed much less sensitivity (0.39 Ω ng^{-1} mL^{-1}). Moreover, a stable EIS response from the Ab/PANI electrode was achieved after only 20 min of incubation (compared to 2 min with Ab/$Cu_3(BTC)_2$/PANI). Hence, the above experiment has clearly outlined the significance of adding $Cu_3(BTC)_2$ in the $Cu_3(BTC)_2$/PANI composite for the efficient biosensing of cTnI.

The results on the investigations on reproducibility of Ab/$Cu_3(BTC)_2$/PANI electrodes are summarized in Fig. 6b. Different batches of the Ab/$Cu_3(BTC)_2$/PANI yielded almost unchanged response, thereby suggesting a good reproducibility of the herein described protocol.

The specificity of the biosensor was also determined (Fig. 7). The system was found to be highly specific to cTnI even in the co-presence of interfering molecules, such as bovine serum albumin (BSA) and ferritin. The Ab/$Cu_3(BTC)_2$/PANI bioelectrodes experienced a change in their R_{ct} values only in the presence of cTnI, while other tested analytes did not influence the sensor response.

A comparative overview of the Ab/$Cu_3(BTC)_2$/PANI and some other previously reported electrochemical sensors for the detection of cTnI is summarized in Table 1. These data clearly indicate about the comparable or better performance of the present biosensor.

3.3. Analysis of spiked sample

The practical utility of the Ab/$Cu_3(BTC)_2$/PANI biosensor has been evaluated by using it for the analysis of mice serum sample spiked with known concentrations of cTnI antigen. The results of the study are presented in Table 2. We observed satisfactory recoveries of the added antigen, highlighting the fact that the Ab/$Cu_3(BTC)_2$/PANI biosensor can also be used in clinical environments.

4. Conclusion

A new MOF based electrochemical biosensor has been developed for highly sensitive and specific quantification of cardiac troponin I. A performance comparison of the Ab/$Cu_3(BTC)_2$/PANI biosensor with the already available biosensors suggests that the system proposed in this study should offer an advanced option for the electrochemical biosensing of cTnI. $Cu_3(BTC)_2$/PANI can be easily synthesized and it bears a large surface area to allow functionalization of high density of antibodies. Due to material characteristics, it should be easy to fabricate the sensor electrode in a more reproducible manner than other nanomaterials like graphene and carbon nanotubes.

Conflicts of interest

The authors declare that they have no conflicts of interest.

Acknowledgements

AG thanks the Department of Biotechnology (DBT), Ministry of Science and Technology, Government of India for her research fellowship. Financial assistance from the projects RRF22/RRF/2018-ISTAD and DST-EMR/2016/006480 is also acknowledged. We also thank Dr Nitin K Singhal (NABI, Mohali, India) for helping in experiments related with the mice serum.

References

1 D. Sun, Z. Luo, J. Lu, S. Zhang, T. Che, Z. Chen, *et al.* Electrochemical dual-aptamer-based biosensor for nonenzymatic detection of cardiac troponin I by nanohybrid electrocatalysts labeling combined with DNA nanotetrahedron structure, *Biosens. Bioelectron.*, 2019, **134**, 49–56.

2 X. Han, S. Li, Z. Peng, A. M. Othman and R. Leblanc, Recent development of cardiac troponin I detection, *ACS Sens.*, 2016, **1**(2), 106–114.

3 G.-J. Zhang, Z. H. H. Luo, M. J. Huang, T. G. Kang and H. Ji, An integrated chip for rapid, sensitive, and multiplexed detection of cardiac biomarkers from fingerprick blood, *Biosens. Bioelectron.*, 2011, **28**(1), 459–463.

4 K.-J. Huang, D.-J. Niu, J.-Y. Sun, C.-H. Han, Z.-W. Wu, Y.-L. Li, *et al.* Novel electrochemical sensor based on functionalized graphene for simultaneous determination of adenine and guanine in DNA, *Colloids Surf., B*, 2011, **82**(2), 543–549.

5 S. K. Tuteja, M. Kukkar, C. Suri, A. Paul and A. Deep, One step in situ synthesis of amine functionalized graphene for immunosensing of cardiac marker cTnI, *Biosens. Bioelectron.*, 2015, **66**, 129–135.

6 M. Panteghini, F. Pagani, K.-T. J. Yeo, F. S. Apple, R. H. Christenson, F. Dati, *et al.* Evaluation of imprecision for cardiac troponin assays at low-range concentrations, *Clin. Chem.*, 2004, **50**(2), 327–332.

7 S. Upasham, A. Tanak and S. Prasad, Cardiac troponin biosensors: where are we now?, *Adv. Healthcare Technol.*, 2018, **4**, 1.

8 H. Jo, H. Gu, W. Jeon, H. Youn, J. Her, S.-K. Kim, *et al.* Electrochemical aptasensor of cardiac troponin I for the early diagnosis of acute myocardial infarction, *Anal. Chem.*, 2015, **87**(19), 9869–9875.

9 X. Liu, H. Liu, M. Li, H. Qi, Q. Gao and C. Zhang, Highly sensitive electrochemiluminescence assay for cardiac troponin I and adenosine triphosphate by using supersandwich amplification and bifunctional aptamer, *Chemelectrochem*, 2017, **4**(7), 1708–1713.

10 S. Kumar, S. Kumar, S. Augustine and B. D. Malhotra, Protein functionalized nanostructured zirconia based electrochemical immunosensor for cardiac troponin I detection, *J. Mater. Res.*, 2017, **32**(15), 2966–2972.

11 W. Zhou, K. Li, Y. Wei, P. Hao, M. Chi, Y. Liu, *et al.* Ultrasensitive label-free optical microfiber coupler biosensor for detection of cardiac troponin I based on interference turning point effect, *Biosens. Bioelectron.*, 2018, **106**, 99–104.

12 S. Dhawan, S. Sadanandan, V. Haridas, N. H. Voelcker and B. Prieto-Simón, Novel peptidylated surfaces for interference-free electrochemical detection of cardiac troponin I, *Biosens. Bioelectron.*, 2018, **99**, 486–492.

13 M. Negahdary, M. Behjati-Ardakani, N. Sattarahmady, H. Yadegari and H. Heli, Electrochemical aptasensing of human cardiac troponin I based on an array of gold nanodumbbells-Applied to early detection of myocardial infarction, *Sens. Actuators, B*, 2017, **252**, 62–71.

14 M. Xu, R. Wang and Y. Li, Electrochemical biosensors for rapid detection of Escherichia coli O157: H7, *Talanta*, 2017, **162**, 511–522.

15 S. Singal, A. K. Srivastava, S. Dhakate and A. M. Biradar, Electroactive graphene-multi-walled carbon nanotube hybrid supported impedimetric immunosensor for the detection of human cardiac troponin-I, *RSC Adv.*, 2015, **5**(92), 74994–75003.

16 S. Singal and A. K. Srivastava, Electrochemical impedance analysis of biofunctionalized conducting polymer-modified graphene-CNTs nanocomposite for protein detection, *Nano-Micro Lett.*, 2017, **9**(1), 7.

17 M. Lakshmanakumar, N. Nesakumar, S. Sethuraman, K. Rajan, U. M. Krishnan and J. B. B. Rayappan, Functionalized graphene quantum dot interfaced electrochemical detection of cardiac troponin I: an antibody free approach, *Sci. Rep.*, 2019, **9**(1), 1–7.

18 F. Chekin, A. Vasilescu, R. Jijie, S. K. Singh, S. Kurungot, M. Iancu, *et al.* Sensitive electrochemical detection of cardiac troponin I in serum and saliva by nitrogen-doped porous reduced graphene oxide electrode, *Sens. Actuators, B*, 2018, **262**, 180–187.

19 T. Kong, R. Su, B. Zhang, Q. Zhang and G. Cheng, CMOS-compatible, label-free silicon-nanowire biosensors to detect cardiac troponin I for acute myocardial infarction diagnosis, *Biosens. Bioelectron.*, 2012, **34**(1), 267–272.

20 A. Gupta, S. K. Bhardwaj, A. L. Sharma, K.-H. Kim and A. Deep, Development of an advanced electrochemical biosensing platform for E. coli using hybrid metal-organic framework/polyaniline composite, *Environ. Res.*, 2019, **171**, 395–402.

21 L. Liu, Y. Zhou, S. Liu and M. Xu, The applications of metal–organic frameworks in electrochemical sensors, *ChemElectroChem*, 2018, **5**(1), 6–19.

22 C.-S. Liu, J. Li and H. Pang, Metal-organic framework-based materials as an emerging platform for advanced electrochemical sensing, *Coord. Chem. Rev.*, 2020, **410**, 213222.

23 X. Fang, B. Zong and S. Mao, Metal–organic framework-based sensors for environmental contaminant sensing, *Nano-Micro Lett.*, 2018, **10**(4), 64.

24 Y. Xu, Q. Li, H. Xue and H. Pang, Metal-organic frameworks for direct electrochemical applications, *Coord. Chem. Rev.*, 2018, **376**, 292–318.

25 Y. Wang, L. Wang, W. Huang, T. Zhang, X. Hu, J. A. Perman, *et al.* A metal–organic framework and conducting polymer based electrochemical sensor for high performance

cadmium ion detection, *J. Mater. Chem. A*, 2017, **5**(18), 8385–8393.

26 S. Shahrokhian and S. Ranjbar, Aptamer immobilization on amino-functionalized metal–organic frameworks: an ultrasensitive platform for the electrochemical diagnostic of Escherichia coli O157: H7, *Analyst*, 2018, **143**(13), 3191–3201.

27 S. K. Bhardwaj, G. C. Mohanta, A. L. Sharma, K.-H. Kim and A. Deep, A three-phase copper MOF-graphene-polyaniline composite for effective sensing of ammonia, *Anal. Chim. Acta*, 2018, **1043**, 89–97.

28 J. Tang, S. Jiang, Y. Liu, S. Zheng, L. Bai, J. Guo, *et al.* Electrochemical determination of dopamine and uric acid using a glassy carbon electrode modified with a composite consisting of a Co (II)-based metalorganic framework (ZIF-67) and graphene oxide, *Microchim. Acta*, 2018, **185**(10), 486.

29 W. Choi, H.-C. Shin, J. M. Kim, J.-Y. Choi and W.-S. Yoon, Modeling and applications of electrochemical impedance spectroscopy (EIS) for lithium-ion batteries, *J. Electrochem. Sci. Eng.*, 2020, **11**, 1–13.

30 X. Yan, S. Komarneni, Z. Zhang and Z. Yan, Extremely enhanced CO2 uptake by HKUST-1 metal–organic framework via a simple chemical treatment, *Microporous Mesoporous Mater.*, 2014, **183**, 69–73.

31 T. Zeng, X. Zhang, Y. Ma, S. Wang, H. Niu and Y. Cai, A functional rattle-type microsphere with a magnetic-carbon double-layered shell for enhanced extraction of organic targets, *Chem. Commun.*, 2013, **49**(54), 6039–6041.

32 Z. Daoben, W. Meixiang, L. Mingzhu, G. Dian and Q. Renyuan, Charge Transfer Complexes of 3, 3′, 5, 5′-Tetra-Phenyl-2, 2′-Dithiodipyranylidine (2, 2′ DIPSØ4) with 7, 7′, 8, 8′-Tetracyanoquinodimethane (TCNQ) And Iodine, *Mol. Cryst. Liq. Cryst.*, 1982, **86**(1), 57–62.

33 K. E. Ramohlola, G. R. Monana, M. J. Hato, K. D. Modibane, K. M. Molapo, M. Masikini, *et al.* Polyaniline-metal organic framework nanocomposite as an efficient electrocatalyst for hydrogen evolution reaction, *Composites, Part B*, 2018, **137**, 129–139.

34 M. Trchová and J. Stejskal, Polyaniline: the infrared spectroscopy of conducting polymer nanotubes (IUPAC Technical Report), *Pure Appl. Chem.*, 2011, **83**(10), 1803–1817.

35 D. Mustafa, E. Breynaert, S. R. Bajpe, J. A. Martens and C. E. Kirschhock, Stability improvement of Cu 3 (BTC) 2 metal–organic frameworks under steaming conditions by encapsulation of a Keggin polyoxometalate, *Chem. Commun.*, 2011, **47**(28), 8037–8039.

36 L. Peng, J. Zhang, Z. Xue, B. Han, X. Sang, C. Liu, *et al.* Highly mesoporous metal–organic framework assembled in a switchable solvent, *Nat. Commun.*, 2014, **5**(1), 1–7.

37 M. Guler, V. Turkoglu and A. Kivrak, Electrochemical detection of malathion pesticide using acetylcholinesterase biosensor based on glassy carbon electrode modified with conducting polymer film, *Environ. Sci. Pollut. Res.*, 2016, **23**(12), 12343–12351.

38 A. Deep, S. K. Bhardwaj, A. Paul, K.-H. Kim and P. Kumar, Surface assembly of nano-metal organic framework on amine functionalized indium tin oxide substrate for impedimetric sensing of parathion, *Biosens. Bioelectron.*, 2015, **65**, 226–231.

39 X. Qin, Y. Sui, A. Xu, L. Liu, Y. Li, Y. Tan, *et al.* Ultrasensitive immunoassay of proteins based on in situ enzymatic formation of quantum dots and microliter-droplet anodic stripping voltammetry, *J. Electroanal. Chem.*, 2018, **811**, 121–127.

40 S. Gomes-Filho, A. Dias, M. Silva, B. Silva and R. Dutra, A carbon nanotube-based electrochemical immunosensor for cardiac troponin T, *Microchem. J.*, 2013, **109**, 10–15.

41 D. Brondani, J. V. Piovesan, E. Westphal, H. Gallardo, R. A. F. Dutra, A. Spinelli, *et al.* A label-free electrochemical immunosensor based on an ionic organic molecule and chitosan-stabilized gold nanoparticles for the detection of cardiac troponin T, *Analyst*, 2014, **139**(20), 5200–5208.